Organic & Biomolecular Chemistry

Cite this: *Org. Biomol. Chem.*, 2012, **10**, 4208

www.rsc.org/obc

PAPER

VCD to determine absolute configuration of natural product molecules: secolignans from *Peperomia blanda*†

Lidiane G. Felippe,‡[a] João M. Batista Jr.,‡*[a] Debora C. Baldoqui,[b] Isabele R. Nascimento,[a] Massuo J. Kato,[c] Yanan He,[d] Laurence A. Nafie[d,e] and Maysa Furlan*[a]

Received 14th January 2012, Accepted 3rd April 2012
DOI: 10.1039/c2ob25109d

The absolute configuration and solution-state conformers of three peperomin-type secolignans isolated from *Peperomia blanda* (Piperaceae) are unambiguously determined by using vibrational circular dichroism (VCD) spectroscopy associated with density functional theory (DFT) calculations. Advantages of VCD over the electronic form of CD for the analysis of diastereomers are also discussed. This work extends our growing knowledge about secondary metabolites within the Piperaceae family species while providing a definitive and straightforward method to assess the absolute stereochemistry of secolignans.

Introduction

The determination of absolute configuration (AC) has often been a difficult stereochemical problem to solve.[1] This is especially critical in the case of natural product molecules which are predominantly chiral and generally enantiomerically enriched.[2] Many methods have been developed over the years to address this problem including X-ray diffraction,[3] NMR methods[4] or stereocontrolled organic synthesis. However, the former requires high quality single crystals whereas the latter is usually laborious, time-consuming, and expensive.[5] Furthermore, none of the methods described above allow direct evaluation of absolute stereochemistry in solution and without derivatization, where the latter may become prohibitive based on the small amounts of natural molecules commonly obtained. As an alternative, chiroptical methods, such as vibrational circular dichroism (VCD), electronic circular dichroism (ECD), Raman optical activity (ROA), and optical rotatory dispersion (ORD), which result from the differential interaction of a chiral molecule with left *versus* right circularly polarized radiation, have gained increasing attention.[6] The confidence in the use of these methods comes from remarkable developments of quantum chemical calculations for reliably predicting vibrational and electronic spectra as well as the availability of user-friendly dedicated instrumentation.

VCD was first described in 1974,[7] confirmed in 1975,[8] and greatly advanced after the advent of Fourier transform VCD in the late 70s,[9] although the first dedicated FT-VCD spectrometer was not brought to market until 1997.[10] VCD is the extension of ECD into infrared and near-infrared regions of the spectrum where vibrational transitions occur within the ground electronic state of the molecule.[1] This technique has many advantages over other methods widely used since there is no need for single crystals, derivatization or UV-vis chromophores, the latter being essential for ECD. Due to the wealth of bands and sensitivity of VCD to molecular conformations, not only is absolute stereochemistry determination feasible but also conformational analysis in solution.[5] By comparing the signs and intensities of the measured VCD spectrum with the corresponding ground electronic state *ab initio* density functional theory (DFT) calculated VCD spectrum of a chosen configuration, one can unambiguously assign the AC of a chiral molecule.[11] The applicability of VCD associated with DFT calculations to AC determination of chiral natural product molecules has been previously demonstrated,[2,10,12–15] including some examples from our research group.[16–18]

Recently, ECD spectroscopy and time-dependent density functional theory (TDDFT) calculations were used to determine the AC of a novel secolignan (**1**) with rare *cis* configuration at the γ-butyrolactone ring, isolated from *Peperomia blanda*,[19] however, other two similar compounds with one additional chiral center each could not be investigated due to limitations inherent to the ECD.

[a]*Organic Chemistry Department, Institute of Chemistry, São Paulo State University – UNESP, Araraquara, SP 14800-900, Brazil. E-mail: maysaf@reitoria.unesp.br, joaombj@hotmail.com; Fax: +55-16-3301-9692; Tel: +55-16-3301-9661*
[b]*Department of Chemistry, Maringá State University, Maringá, PR, 87020-900, Brazil*
[c]*Department of Fundamental Chemistry, Institute of Chemistry, University of São Paulo, SP 05508-000, Brazil*
[d]*BioTools, Inc. Jupiter, FL 33458, USA*
[e]*Department of Chemistry, Syracuse University, Syracuse, NY 13244-4100, USA*

†Electronic supplementary information (ESI) available: Molecular modeling of **2** and **3**, ^{1}H NMR, ^{13}C NMR, *g*COSY, *g*HMQC, *g*HMBC, 1D NOESY, HRESIMS spectra of **3**, 1D NOESY spectra of **2**. See DOI: 10.1039/c2ob25109d

‡These authors contributed equally to this manuscript as first authors.

Peperomia blanda (Jacq.) H.B. & K. belongs to Piperaceae family and is a perennial herb that typically grows in wet rock crevices and is found from the northeast to the south of Brazil.[20] Although predominantly used as ornamental plants,[21] some members of *Peperomia* genus containing secolignans are widely used in traditional Chinese medicine to treat various types of cancer.[22–24] Despite its importance, most of the secolignans reported in the literature have their AC only partially assigned by comparison with OR and/or empirical ECD data of similar compounds, with exceptions commonly present.[1,16,25,26] In the work presented here we expand the studies with a special class of bioactive secolignans, known as peperomins, with the application of VCD spectroscopy and DFT calculations to confirm the previous assignment of **1** and to determine unambiguously the absolute configuration of two new diastereomers, **2** and **3**, which remained undetermined. This is the first time that compound **2** has been isolated from *P. blanda* and the first time compound **3** is described in nature.

Therefore, this work will help extend our growing knowledge about secondary metabolites within the Piperaceae family species, while providing a definitive method to assess the absolute stereochemistry and solution-state conformations of secolignans.

Results and discussion

Secolignans **1–3** (Fig. 1) were obtained from the EtOAc extract of the aerial parts of *Peperomia blanda*. Compound **1** was isolated according to methodology previously described.[19] The EtOAc extract was further subjected to CC over silica gel followed by preparative HPLC to afford compounds **2** and **3**. Their structures were elucidated by a combination of spectroscopic methods, including ultraviolet, infrared, 1D- and 2D-nuclear magnetic resonance (NMR) as well as high resolution mass spectrometry data. Compound **1** was identified as (2*R*,3*S*)-2-methyl-3-[bis(3′,4′-methylenedioxy-5′-methoxyphenyl)methyl]butyrolactone previously reported from *P. blanda*,[19] and compound **2** was suggested to be the known secolignan peperomin B, initially described from *P. japonica*.[27] The relative configuration of **2** was determined by 1D NOESY experiments. The *trans* configuration at the γ-butyrolactone ring of **2** was established by irradiation of H-3, which resulted in an NOE enhancement for $-CH_3$-6. Additionally, upon irradiation of H-5 an NOE enhancement was observed for H-2. Furthermore, irradiation of H-2″/6″ and H-4a resulted in NOE enhancement for H-2 and H-2′, respectively. The molecular formula of the novel compound **3** was established as $C_{23}H_{26}O_8$ by HRMS ([M + Na]$^+$ obsd *m/z* 453.1518, calcd 453.1519) in combination with extensive NMR analysis. The ^{1}H NMR spectrum (Table 1) exhibited resonances of two *meta*-coupled aromatic hydrogens at δ 6.31 (d, H-6′, J = 1.5 Hz) and 6.34 (d, H-2′, J = 1.5 Hz), two chemically equivalent hydrogens at δ 6.42 (s, H-2″ and H-6″), one methylenedioxy group at δ 5.84 (d, J = 1.5 Hz) and 5.86 (d, J = 1.5 Hz), and three *O*-methyl singlets at δ 3.75 (4″–OCH_3), 3.79 (3″–OCH_3 and 5″–OCH_3), and 3.83 (5′-OCH3). A doublet at δ 1.04 (H-6, J = 7.5 Hz) was assigned to the methyl group at C-2, and signals at δ 3.97 (dd, H-4a, J = 9.0 and 10.0 Hz), 3.86 (br t, H-4b, J = 10.0 Hz), due to the methylene group of the butyrolactone moiety, as well as a quintet at δ 2.65 (H-2, J = 7.5 Hz), a multiplet at 3.30 (H-3), and a doublet at δ 3.64 (H-5, J = 12.0 Hz), due to three methine groups, were also observed. A γ-butyrolactone ring was confirmed by the *g*HMBC and *g*HMQC cross-peaks between H-2, H-4, and H-6 and the lactone carbonyl carbon [δ 179.9 (C-1)]. The ^{13}C NMR data corroborated the presence of the butyrolactone system, and all signals were accordingly assigned based on the *g*HMBC data (Table 1). The relative configuration of **3** was also determined by 1D NOESY experiments. The *cis* configuration at the γ-butyrolactone ring was established by irradiation of H-3, which resulted in an NOE enhancement for H-2. Additionally, upon irradiation of H-5 an NOE enhancement was observed for $-CH_3$-6. Furthermore, irradiation of H-2″/6″ and H-2′ resulted in NOE enhancement for H-2 and H-4b, respectively. The absolute configuration of each secolignan was determined by comparing the experimental IR and VCD spectra with the output of quantum chemistry calculations.

As for compound **1**, a thorough conformational analysis was carried out when its structure and absolute configuration by ECD

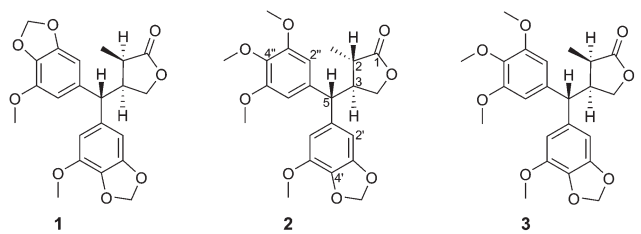

Fig. 1 Structure of secolignans **1–3** from the aerial parts of *Peperomia blanda*.

Table 1 NMR data of compounds **2** and **3** ($CDCl_3$, 11.7 T)

	2		**3**	
Position	^{1}H (δ)[a]	^{13}C (δ)	^{1}H (δ)[a]	^{13}C (δ)
1		179.5		179.9
2	2.28 qn (7.5)	40.2	2.65 qn (7.5)	37.7
3	2.83 m	47.2	3.30 m	43.0
4a	4.24 dd (2.0, 8.0)	70.2	3.97 dd (9.0, 10.0)	70.4
4b	3.77 ov[b]		3.86 br t (10.0)	
5	3.55 d (11.5)	56.3	3.64 d (12.0)	50.4
6	0.88 d (7.5)	15.8	1.04 d (7.5)	10.4
1′		136.1		137.2
2′	6.42 d (1.5)	101.2	6.34 d (1.5)	101.0
3′		149.5		149.4
4′		134.3		134.3
5′		143.6		143.5
6′	6.35 d (1.5)	108.1	6.31 d (1.5)	107.5
1″		137.5		137.3
2″ and 6″	6.39 s	104.9	6.42 s	104.4
3″		153.5		153.6
4″		137.4		136.5
5″		153.5		153.6
3′,4′-OCH_2O	5.87 d (1.5)	101.4	5.84 d (1.5)	101.4
	5.88 d (1.5)		5.86 d (1.5)	
5′-OCH_3	3.85 s	57.0	3.83 s	57.0
3″-OCH_3	3.78 s	56.3	3.79 s	56.3
4″-OCH_3	3.74 s	60.8	3.75 s	60.8
5″-OCH_3	3.78 s	56.3	3.79 s	56.3

[a] Signals were assigned with the assistance of ^{1}H–^{1}H *g*COSY experiments, J in Hz. [b] Overlapped.

were first described.[19] Based on that, the same lowest-lying optimized conformers identified, which differed mainly with respect to the relative positioning of the aromatic rings and their substituents, were now considered for IR and VCD spectral simulation. The excellent agreement between observed and calculated (B3LYP/6-31G(d)) data (Fig. 2) allowed us to confirm the absolute configuration of (−)-**1** as (2*R*,3*S*).

Compound **2** differs from **1** and **3** mainly with regard to its *trans* configuration at the γ-butyrolactone ring (Fig. 1). Analysis of spectroscopic data confirmed **2** to have the same structure and relative configuration at the butyrolactone ring as peperomin B,[27] which has never been described in *P. blanda*. The first time peperomin B was reported,[27] a positive optical rotation, associated with positive and negative Cotton effects at approximately 275 and 250 nm, respectively, led to the assignment of its AC as (2*S*,3*S*,5*S*). Upon comparing the experimental data obtained for **2** with literature values, we realized that despite very similar optical rotation ($[\alpha]_D^{21}$ +21.8° [dm g cm^{-3}]$^{-1}$ ($CHCl_3$; *c* 0.49)), the ECD data was not consistent with those reported previously for peperomin B. Even though a positive Cotton effect was observed at 275 nm it was followed by a slightly negative and a strong positive Cotton effect at 260 and 240 nm, respectively. These discrepancies between our experimental results and the literature values prompted us to calculate the ECD spectrum of **2** using time-dependent DFT (TDDFT). The eight lowest-energy optimized conformers identified for both (2*S*,3*S*,5*S*)- and (2*S*,3*S*,5*R*)-**2** (see ESI†), which differ mainly with respect to the relative positioning of the aromatic rings and their substituents, were considered for ECD spectral simulation. This approach permitted us to probe all possible configurations within the three existing chiral centers, taking into account the *trans* configuration at the γ-butyrolactone ring. The antipodes of the arbitrarily chosen configurations were generated by multiplying their final spectra by (−1).

The comparison of experimental and calculated (B3LYP/6-311G++(2d,2p)//B3LYP/6-31G(d)) ECD spectra of **2** is presented in Fig. 3. From that, it is possible to observe that both (2*S*,3*S*,5*S*)- and (2*S*,3*S*,5*R*)-**2** calculated spectra are in good agreement with experimental data. Therefore, ECD cannot be used to determine unambiguously the absolute configuration of **2** since it is not capable of differentiating C-5 diastereomers. This fact may arise from the similarity of the two aromatic substituents at the putative chiral center, which share basically the same electronic transition properties. Additionally, ECD is referred to as a lower resolution technique compared to VCD, exhibiting fewer and broader bands.

Thus, VCD constitutes a good alternative to ECD since it arises from chiral interactions of vibrations of molecular bonds (nuclear motions) and its sensitivity to minor structural changes provides a higher level of analytical power to elucidate absolute molecular structure, provided conformational flexibility is addressed accordingly. For that reason, the next step was to calculate the IR and VCD spectra of the same diastereomers considered in the ECD analysis and compare them with experimental results. Indeed, VCD provided a definitive assignment of

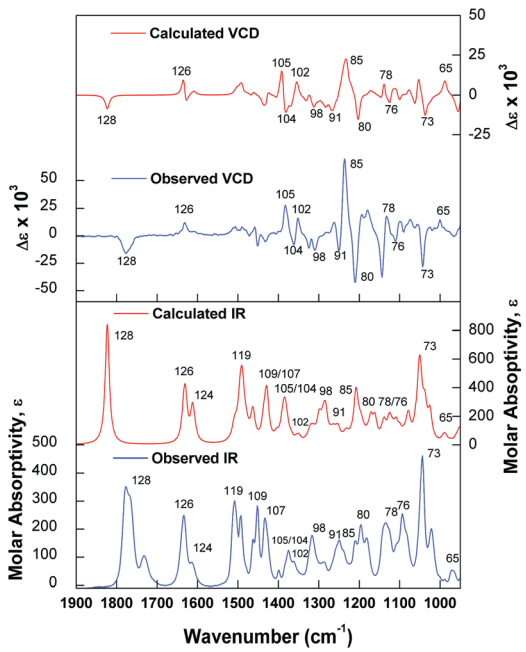

Fig. 2 Comparison of the VCD and IR spectra of the measured (−)-**1** with the calculated [B3LYP/6-31G(d)] VCD and IR spectra of the Boltzmann average of the seven lowest-energy conformers of the corresponding (2*R*,3*S*)-**1**. The comparison establishes the absolute configuration of this molecule as (−)-(2*R*,3*S*)-**1**. Numbers represent fundamental vibrational modes.

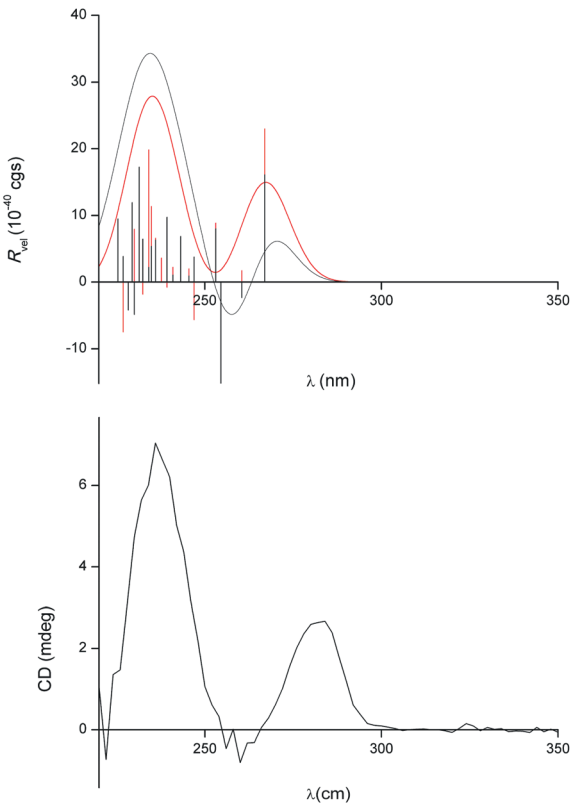

Fig. 3 Comparison of the ECD spectrum of the measured (+)-**2** (lower frame) with the calculated [B3LYP/6-311G++(2d,2p)//B3LYP/6-31G(d)] ECD spectra of the Boltzmann average of the eight lowest-energy conformers of the corresponding (2*S*,3*S*,5*S*)-**2** (upper frame red) and (2*S*,3*S*,5*R*)-**2** (upper frame black). Bars represent rotational strengths for the weighted ECD spectra.

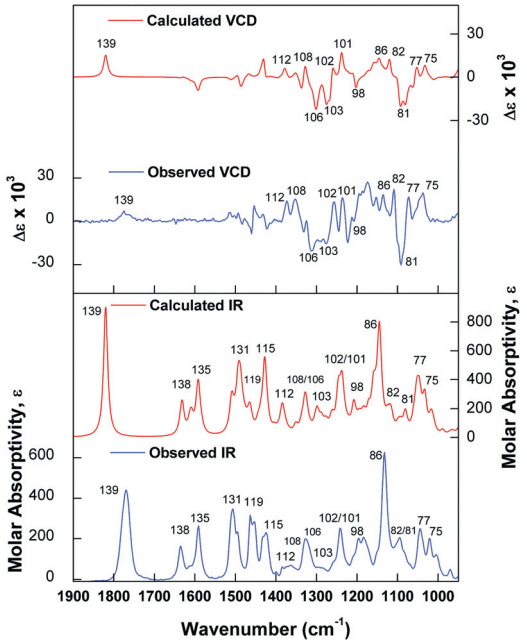

Fig. 4 Comparison of the VCD and IR spectra of the measured (+)-**2** with the calculated [B3LYP/6-31G(d)] VCD and IR spectra of the Boltzmann average of the eight lowest-energy conformers of the corresponding (2*S*,3*S*,5*S*)-**2**. The comparison establishes the absolute configuration of this molecule as (+)-(2*S*,3*S*,5*S*)-**2**. Numbers represent fundamental vibrational modes.

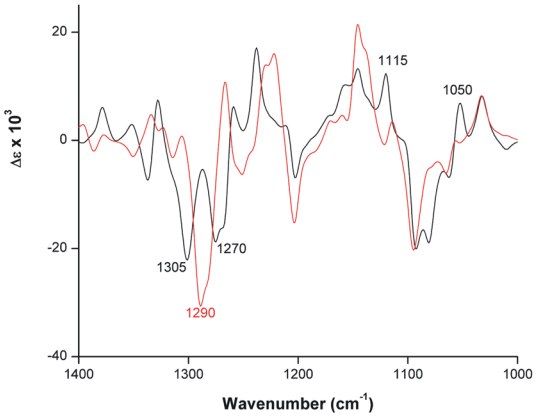

Fig. 5 Superposition of the calculated [B3LYP/6-31G(d)] VCD spectra of the Boltzmann average of the eight lowest-energy conformers of the corresponding (2*S*,3*S*,5*S*)-**2** (black) and (2*S*,3*S*,5*R*)-**2** (red). Numbers represent distinct vibrational transitions between the two diastereomers used to assign the absolute configuration of (+)-**2** as (2*S*,3*S*,5*S*).

$(+)_{589}$-**2** as (2*S*,3*S*,5*S*) (Fig. 4). Therefore, compound **2** was confirmed to be peperomin B.[27] In spite of the same overall shape, the VCD spectra of the diastereomers (2*S*,3*S*,5*S*)- and (2*S*,3*S*,5*R*)-**2** presented some distinct features which led to the correct assignment (Fig. 5). The vibrational transitions at 1270 and 1305 cm^{-1} present in (2*S*,3*S*,5*S*)-**2** and replaced by a single transition at 1290 cm^{-1} in (2*S*,3*S*,5*R*)-**2** were crucial to distinguishing between the epimers. Such transitions represent mainly bending vibrations involving the C–H group at the chiral center C-5. Finally, for the assignment of (+)-(2*S*,3*S*,5*S*)-**2** the output of the confidence level algorithm[28] was $\Delta = 66.2$ and confidence level of 100%, whereas for the diastereomer (2*S*,3*S*,5*R*)-**2** it was $\Delta = 47.8$ with a confidence level of 78%.

For compound **3**, the same approach was used in order to determine its AC. As this is the first time this secondary metabolite is described in nature, there was no appropriate model to which its ECD spectrum could be compared. Thus we proceeded with the construction of the computational model, conformational search, geometry optimization, and simulation of both ECD and VCD spectra. As a result eight lowest-energy conformers were identified at the B3LYP/6-31G(d) (see ESI†) level and used to create the Boltzmann-weighted composite ECD and VCD spectra. Once again, the TDDFT-calculated ECD (B3LYP/6-311G++(2d,2p)) spectra for the two diastereomers possible at C-5, taking into account now the *cis* relative configuration at the γ-butyrolactone ring, were basically identical, thus preventing the unambiguous assignment of the absolute configuration of (−)-**3** (Fig. 6). Even though compounds **1** and **3** possess the same *cis* relative configuration at the butyrolactone ring as well as the same sign and comparable magnitude of the optical

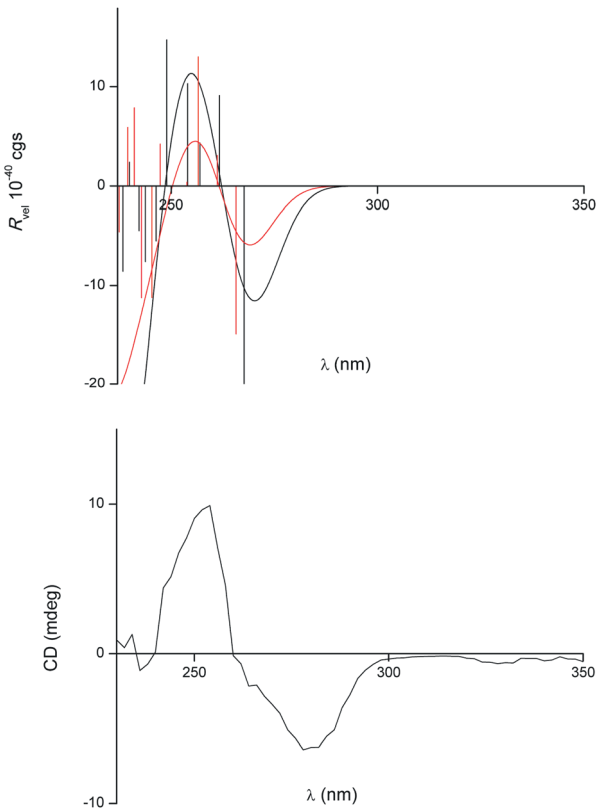

Fig. 6 Comparison of the ECD spectrum of the measured (−)-**3** (lower frame) with the calculated [B3LYP/6-311G++(2d,2p)//B3LYP/6-31G(d)] ECD spectra of the Boltzmann average of the eight lowest-energy conformers of the corresponding (2*R*,3*S*,5*S*)-**3** (upper frame red) and (2*R*,3*S*,5*R*)-**3** (upper frame black). Bars represent rotational strengths for the weighted ECD spectra.

rotation, compound **3** presents one additional chiral center and must not be directly compared with **1**.

Interestingly, the calculated IR and VCD at the B3LYP/6-31G(d) level were not accurate enough to differentiate diastereomers, so

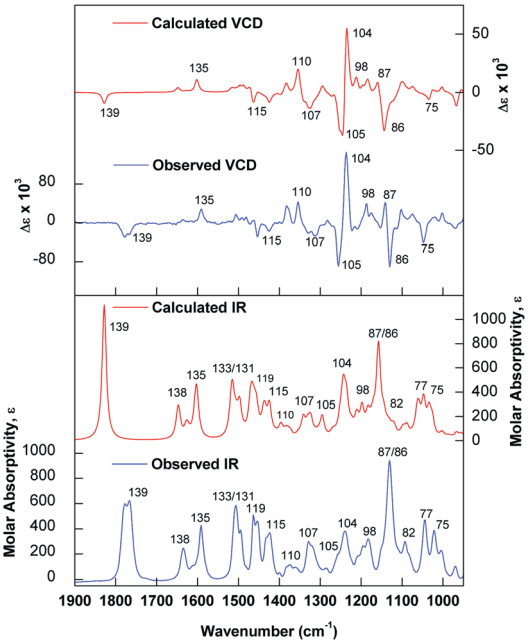

Fig. 7 Comparison of the VCD and IR spectra of the measured (−)-**3** with the calculated [B3PW91/TZVP] VCD and IR spectra of the Boltzmann average of the eight lowest-energy conformers of the corresponding (2*R*,3*S*,5*S*)-**3**. The comparison establishes the absolute configuration of this molecule as (−)-(2*R*,3*S*,5*S*)-**3**. Numbers represent fundamentals.

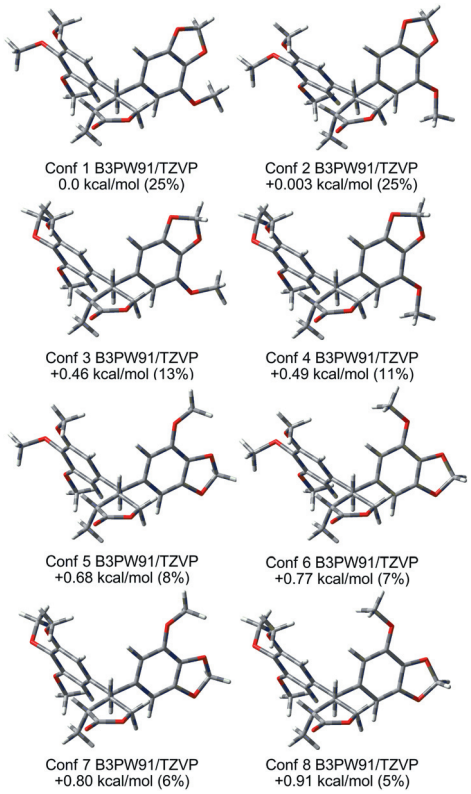

Fig. 8 Optimized structures and relative energy of the eight lowest-energy conformers of (2*R*,3*S*,5*S*)-**3** at the B3PW91/TZVP level.

we decided to recalculate the spectra using a larger basis set (TZVP), which uses a Gaussian basis set of triple ζ valence quality augmented by polarization functions, and the B3PW91 hybrid functional.[29] Indeed, the new calculations generated a much better result and allowed the assignment of (−)-**3** as (2*R*,3*S*,5*S*). The comparison of experimental and calculated (B3PW91/TZVP) VCD spectra for **3** and the lowest-energy conformers identified, which differ mainly with respect to the relative positioning of the aromatic rings and their substituents, are presented in Fig. 7 and 8, respectively.

In this case, both diastereomers presented the same overall shape for their IR and VCD spectra, however the vibrational transitions at 1210 and 1240 cm^{-1} (Fig. 9), which correspond to bending vibrations involving the C–H group as well as the other substituents bonded to the stereogenic carbon C-5, were critical for the assignment of (−)-**3** as (2*R*,3*S*,5*S*). For this assignment the output of the confidence level algorithm was Δ = 67.9 and confidence level of 100%.

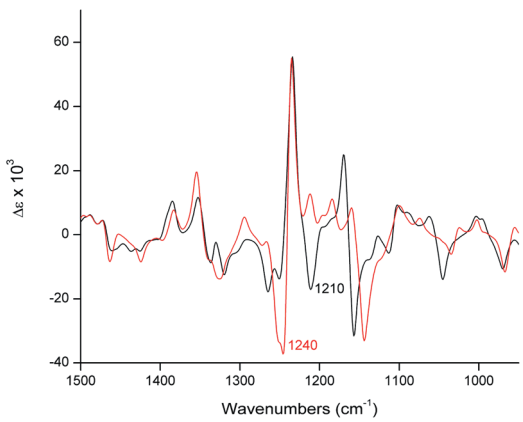

Fig. 9 Superposition of the calculated [B3PW91/TZVP] VCD spectra of the Boltzmann average of the eight lowest-energy conformers of the corresponding (2*R*,3*S*,5*R*)-**3** (black) and (2*R*,3*S*,5*S*)-**3** (red). Numbers represent distinct vibrational transitions between the two diastereomers used to assign the absolute configuration of (−)-**3** as (2*R*,3*S*,5*S*).

Conclusion

Comparison of experimental and calculated IR and VCD spectra of three secolignans isolated from *P. blanda* (Piperaceae) established their AC and conformer distributions directly in $CDCl_3$ solution. This is the first time that compound **2** is reported from *P. blanda* and that compound **3** is described in nature. The advantages of using VCD over ECD to determining the AC of diastereomeric natural product molecules were clearly demonstrated. The three compounds were assigned as follows: (−)-(2*R*,3*S*)-**1**, (+)-(2*S*,3*S*,5*S*)-**2**, and (−)-(2*R*,3*S*,5*S*)-**3**. For those molecules with the rare *cis* relative configuration at the γ-butyrolactone ring, namely **1** and **3**, the same absolute configuration (2*R*,3*S*) was found which may suggest that their formations proceed *via* the same biosynthetic pathway. Therefore, this work extends our growing knowledge about secondary metabolites within the Piperaceae family species while providing a definitive and straightforward method to assess absolute stereochemistry of secolignans.

Experimental

General

One-dimensional (^{1}H, ^{13}C, DEPT, and *g*NOESY) and two-dimensional (*g*COSY, *g*HMBC and *g*HMQC) were recorded on a Varian Inova-500 (11.7 T) spectrometer at 500 MHz (^{1}H) and 125 MHz (^{13}C) using $CDCl_3$ as solvent and TMS as reference. HRESIMS was measured using a Bruker Daltonics model ultrO-TOF$_Q$ ESI-TOF instrument. The optical rotations were measured in $CHCl_3$ at 589 nm in a digital polarimeter JASCO model DIP-370, and the UV spectra recorded in MeOH using an HP 8452 A spectrophotometer. Separations by column chromatography (CC) were carried out using silica gel (230–400 mesh; Merck). All solvents were redistilled prior to use. HPLC separations were performed on a Varian PrepStar model SD-1 LC/UV-vis chromatograph equipped with a Phenomenex C-18 reversed phase column (250 × 21.2 mm). IR and VCD spectra of **1–3** were recorded with a Dual-PEM Chiral*IR*-2X™ FT-VCD spectrometer (BioTools, Jupiter, FL) using a resolution of 4 cm^{-1} and a collection time of 12 h. The optimum retardation of the two ZnSe photoelastic modulators (PEMs) was set at 1400 cm^{-1}. VCD spectra were measured with the dual-PEM option by subtracting in real time the VCD spectra associated with each of the two PEMs as previously described.[30] Spectra were calibrated automatically, using the standard calibration files. Minor instrumental baseline offsets were eliminated from the final VCD spectra by subtracting the VCD spectra of **1–3** from that obtained for the solvent under the same conditions. VCD spectra were recorded in $CDCl_3$ solution (6.5 mg of **1** in 100 μL of $CDCl_3$, 5.0 mg of **2** in 100 μL of $CDCl_3$, and 6.3 mg of **3** in 200 μL of $CDCl_3$, all in a BaF_2 cell with 100 μm path length). The ECD spectra of each compound eluting from the HPLC were measured in the Jasco CD-2095 detector by trapping in a 1.0 cm quartz cell through a switching valve. The spectra were average computed over three instrumental scans and the intensities are presented in terms of ellipticity values (mdeg). The ECD spectra were corrected by baseline subtraction obtained from a measurement of the same solvent used (acetonitrile–H_2O 50 : 50 + 0.5% formic acid).

Plant material

The aerial parts of *Peperomia blanda* (Jacq.) H.B. & K. were collected at Reserva da Ripasa, Ibaté – SP, Brazil in January of 2008 and identified by Dra. Elsie Franklin Guimarães. A voucher specimen (Kato-547) has been deposited at the Herbarium of the Instituto de Biociências, Universidade de São Paulo, São Paulo – SP, Brazil.

Isolation of compounds

Dried aerial parts (86 g) of *P. blanda* were milled, extracted with EtOAc, and the extract concentrated under vacuum to yield 8.5 g. The extract was resuspended in MeOH–H_2O (4 : 1) and partitioned with hexanes, CH_2Cl_2, and EtOAc, successively. The portion soluble in CH_2Cl_2 (1.95 g) was subjected to CC over silica gel and eluted with a gradient of hexanes–EtOAc to yield fractions 1–14. Fraction 10 (0.875 g) was subjected to preparative HPLC and eluted with isocratic MeOH–H_2O (1 : 1) at a flow rate of 13 mL min^{-1} to afford compounds **2** (69.4 mg, t_R = 34.2 min) and **3** (60.5 mg, t_R = 31.2 min). The enantiomeric excess (ee > 95%) for each compound was determined by HPLC using commercial analytical chiral column Chiralcel OD-RH (250 × 4.6 mm, 5 μm, 50% ACN–H_2O with 0.5% formic acid, 0.7 mL min^{-1}, 280 nm).

Computational methods

All DFT and TDDFT calculations were carried out at 298 K in gas phase with Gaussian 09.[31] Regarding compound **1**, the steps of conformational search and geometry optimization were previously described.[19] As for compounds **2** and **3**, calculations were performed for the arbitrarily chosen (2*S*,3*S*,5*S*)- and (2*S*,3*S*,5*R*)-**2** as well as (2*R*,3*S*,5*S*)- and (2*R*,3*S*,5*R*)-**3**. Conformational searches were carried out at the molecular mechanics level of theory employing MM+ and MMFF force fields incorporated in Hyperchem 7 and Spartan 08 software packages, respectively. For (2*S*,3*S*,5*R*)-**2**, 31 conformers with relative energy (rel E.) within 6 kcal mol^{-1} of the lowest-energy conformer were selected and further geometry optimized at the B3LYP/6-31G(d) level. Among the 11 conformers with rel E. <1.5 kcal mol^{-1}, the eight lowest-energy conformers, which correspond to 85% of the total Boltzmann distribution, were selected for ECD and VCD spectral calculation. The same eight lowest-energy conformers identified for (2*S*,3*S*,5*R*)-**2** were then used to create its diastereomer (2*S*,3*S*,5*S*)-**2**, by inverting the chiral centre at C-5. These conformers were further geometry optimized at the same level of theory. The Boltzmann factor for each conformer was calculated based on Gibbs free energy. Vibrational analysis at the B3LYP/6-31G(d) level resulted in no imaginary frequencies, confirming the considered conformers as real minima. TDDFT was employed to calculate excitation energy (in nm) and rotatory strength *R* in dipole velocity (R_{vel} in cgs units: 10^{-40} erg esu cm Gauss^{-1}) form, at the B3LYP/6-311G++(2d,2p) level. The calculated rotatory strengths from the first 20 singlet → singlet electronic transitions were simulated into an ECD curve using Gaussian band shapes and 10 nm half-width at 1/*e* of peak height. The predicted wavelength transitions were used as such without any scaling. IR and VCD spectra for both **1** and **2** were created using dipole and rotational strengths from Gaussian, which were calculated at the B3LYP/6-31G(d) level and converted into molar absorptivities (M^{-1} cm^{-1}). Each spectrum was plotted as a sum of Lorentzian bands with half-widths of 6 cm^{-1}. The calculated wavenumbers were multiplied with a scaling factor of 0.97 and the Boltzmann-population-weighted composite spectra were plotted using Origin software. For (2*R*,3*S*,5*R*)-**3**, 32 conformers with rel E. within 6 kcal mol^{-1} of the lowest-energy conformer were selected and further geometry optimized at the B3LYP/6-31G(d) level. Among the 16 conformers with rel E. <1.5 kcal mol^{-1}, the eight lowest-energy conformers, which correspond to 75% of the total Boltzmann distribution, were selected for ECD and VCD spectral calculation. The same eight lowest-energy conformers identified for (2*R*,3*S*,5*R*)-**3** were then used to create its diastereomer (2*R*,3*S*,5*S*)-**3**, by inverting the chiral centre at C-5. These conformers were further geometry optimized at the same level of theory. The Boltzmann factor for each conformer was calculated

based on Gibbs free energy. Vibrational analysis at the B3LYP/6-31G(d) level resulted in no imaginary frequencies, confirming the considered conformers as real minima. TDDFT was also employed to calculate excitation energy (in nm) and rotatory strength R in dipole velocity (R_{vel} in cgs units: 10^{-40} erg esu cm Gauss^{-1}) form, at the B3LYP/6-311G++(2d,2p) level. The calculated rotatory strengths from the first 10 singlet → singlet electronic transitions were simulated into an ECD curve using Gaussian band shapes and 10 nm half-width at 1/e of peak height. Initially, IR and VCD spectra for **3** were created using dipole and rotational strengths calculated at the B3LYP/6-31G(d) level. However, for the final IR and VCD spectral simulation, the lowest-lying conformers were further geometry optimized using the model chemistry B3PW91/TZVP and the dipole and rotational strengths were calculated at the same level of theory. The predicted wavenumbers were then multiplied with a scaling factor of 0.98 and the final spectra plotted as a sum of Lorentzian bands with half-widths of 6 cm^{-1}.

(2*R*,3*S*,5*S*)-2-Methyl-3-[5(3′,4′-methylenedioxy-5′ methoxyphenyl)-5-(3′,4′,5′-trimethoxyphenyl)metil]butyrolactone (3)

Pale yellow oil, $[\alpha]_D^{21}$ −55.3° [dm g cm^{-3}]$^{-1}$ ($CHCl_3$; *c* 0.49). UV (MeOH) λ_{max}: 224, 247, 275 nm. ^{1}H and ^{13}C NMR see Table 1. HRMS/ESI-TOF *m/z* (rel. int.): 453.1518 [M + Na]$^+$ (98), (calcd for $C_{23}H_{26}O_8Na$, 453.1519).

Acknowledgements

The authors thank BioTools, Inc. for the VCD measurements as well as Prof. Daniel Rinaldo and Prof. Wagner Vilegas for ECD measurements. This work was supported with grants provided by the State of São Paulo Research Foundation (FAPESP 2009/51850-9). JMBJ thanks FAPESP for the provision of a scholarship 2008/58658-3. LGF thanks CAPES for providing scholarship. This research was also supported by resources supplied by the Center for Scientific Computing (NCC/GridUNESP) of the São Paulo State University (UNESP). MJK and MF are also grateful to CNPq for research fellowships.

Notes and references

1 T. B. Freedman, X. Cao, R. K. Dukor and L. A. Nafie, *Chirality*, 2003, **15**, 743.
2 P. J. Stephens, F. J. Devlin and J. J. Pan, *Chirality*, 2008, **20**, 643.
3 H. D. Flack and G. Bernardinelli, *Chirality*, 2008, **20**, 681.
4 J. M. Seco, E. Quiñoá and R. Riguera, *Chem. Rev.*, 2004, **104**, 17.
5 J. Sadlej, J. C. Dobrowolski and J. E. Rode, *Chem. Soc. Rev.*, 2010, **39**, 1478.
6 P. L. Polavarapu, *Chirality*, 2008, **20**, 664.
7 G. Holzwarth, E. C. Hsu, H. S. Mosher, T. R. Faulkner and A. Moscowitz, *J. Am. Chem. Soc.*, 1974, **96**, 251.
8 L. A. Nafie, J. C. Cheng and P. J. Stephens, *J. Am. Chem. Soc.*, 1975, **97**, 3842.
9 L. A. Nafie, M. Diem and D. W. Vidrine, *J. Am. Chem. Soc.*, 1979, **101**, 496.
10 L. A. Nafie, *Nat. Prod. Commun.*, 2008, **3**, 451.
11 Y. He, B. Wang, R. K. Dukor and L. A. Nafie, *Appl. Spectrosc.*, 2011, **65**, 699.
12 F. J. Devlin, P. J. Stephens, J. R. Cheeseman and M. J. Frisch, *J. Phys. Chem. A*, 1997, **101**, 6322.
13 C. M. Cerda-García-Rojas, H. A. García-Gutiérrez, J. D. Hernández-Hernández, L. U. Román-Marín and P. Joseph-Nathan, *J. Nat. Prod.*, 2007, **70**, 1167.
14 E. Burgueño-Tapia, L. G. Zeped and P. Joseph-Nathan, *Phytochemistry*, 2010, **71**, 1158.
15 M. A. Gómez-Hurtado, J. M. Torres-Valencia, J. Manríquez-Torres, R. E. del Río, V. Motilva, S. García-Mauriño, J. Ávila, E. Talero, C. M. Cerda-García-Rojas and P. Joseph-Nathan, *Phytochemistry*, 2011, **72**, 409.
16 J. M. Batista, A. N. L. Batista, D. Rinaldo, W. Vilegas, Q. B. Cass, V. S. Bolzani, M. J. Kato, S. N. López, M. Furlan and L. A. Nafie, *Tetrahedron: Asymmetry*, 2010, **21**, 2402.
17 J. M. Batista, A. N. L. Batista, J. S. Mota, Q. B. Cass, M. J. Kato, V. S. Bolzani, T. B. Freedman, S. N. López, M. Furlan and L. A. Nafie, *J. Org. Chem.*, 2011, **76**, 2603.
18 J. M. Batista, A. N. L. Batista, D. Rinaldo, W. Vilegas, D. L. Ambrósio, R. M. B. Cicarelli, V. S. Bolzani, M. J. Kato, L. A. Nafie, S. N. López and M. Furlan, *J. Nat. Prod.*, 2011, **74**, 1154.
19 L. G. Felippe, J. M. Batista, D. C. Baldoqui, I. R. Nascimento, M. J. Kato, V. S. Bolzani and M. Furlan, *Phytochem. Lett.*, 2011, **4**, 245.
20 E. F. Guimarães and L. C. S. Giordano, *Rodriguésia*, 2004, **55**, 21.
21 J. S. Mota, A. C. Leite, J. M. Batista, S. N. López, D. L. Ambrósio, G. D. Passerini, M. J. Kato, V. S. Bolzani, R. M.B. Cicarelli and M. Furlan, *Planta Med.*, 2009, **75**, 620.
22 C. M. Chen, F. Y. Jan, M. T. Chen and T. J. Lee, *Heterocycles*, 1989, **29**, 411.
23 N. Li, J. L. Wu, J. I. Sakai and M. Ando, *J. Nat. Prod.*, 2003, **66**, 1421.
24 J. L. Wu, N. Li, T. Hasegawa, J. I. Sakai, T. Mitsui, H. Ogura, T. Kataoka, S. Oka, M. Kiuchi, A. Tomida, T. Turuo, M. Li, W. Tang and M. Ando, *J. Nat. Prod.*, 2006, **69**, 790.
25 J. M. Batista, S. N. López, J. S. Mota, K. L. Vanzolini, Q. B. Cass, D. Rinaldo, W. Vilegas, V. S. Bolzani, M. J. Kato and M. Furlan, *Chirality*, 2009, **21**, 799.
26 S. Xu, N. Li, M.-M. Ning, C.-H. Zhou, Q.-R. Yang and M.-W. Wang, *J. Nat. Prod.*, 2006, **69**, 247.
27 C. M. Chen, F. Y. Jan, M. T. Chen and T. J. Lee, *Heterocycles*, 1989, **29**, 411.
28 E. Debie, E. De Gussem, R. K. Dukor, W. Herrebout, L. A. Nafie and P. Bultinck, *ChemPhysChem*, 2011, **12**, 1542.
29 F. Weigend and R. Ahlrichs, *Phys. Chem. Chem. Phys.*, 2005, **7**, 3297.
30 L. A. Nafie, *Appl. Spectrosc.*, 2000, **54**, 1634.
31 M. J. Frisch, G. W. Trucks, H. B. Schlegel, G. E. Scuseria, M. A. Robb, J. R. Cheeseman, G. Scalmani, V. Barone, B. Mennucci, G. A. Petersson, H. Nakatsuji, M. Caricato, X. Li, H. P. Hratchian, A. F. Izmaylov, J. Bloino, G. Zheng, J. L. Sonnenberg, M. Hada, M. Ehara, K. Toyota, R. Fukuda, J. Hasegawa, M. Ishida, T. Nakajima, Y. Honda, O. Kitao, H. Nakai, T. Vreven, J. A. Montgomery Jr., J. E. Peralta, F. Ogliaro, M. Bearpark, J. J. Heyd, E. Brothers, K. N. Kudin, V. N. Staroverov, R. Kobayashi, J. Normand, K. Raghavachari, A. Rendell, J. C. Burant, S. S. Iyengar, J. Tomasi, M. Cossi, N. Rega, J. M. Millam, M. Klene, J. E. Knox, J. B. Cross, V. Bakken, C. Adamo, J. Jaramillo, R. Gomperts, R. E. Stratmann, O. Yazyev, A. J. Austin, R. Cammi, C. Pomelli, J. W. Ochterski, R. L. Martin, K. Morokuma, V. G. Zakrzewski, G. A. Voth, P. Salvador, J. J. Dannenberg, S. Dapprich, A. D. Daniels, O. Farkas, J. B. Foresman, J. V. Ortiz, J. Cioslowski and D. J. Fox, *GAUSSIAN 09 (Revision A.02)*, Gaussian, Inc., Wallingford CT, 2009.

